A New Microwave Oscillator-Based Microfluidic Sensor for Complex Permittivity Measurement

Chu-Hsuan Pai[1], Chao-Hsiung Tseng[2]
Department of Electronic and Computer Engineering,
National Taiwan University of Science and Technology, Taiwan
[1]vivi00077@gmail.com, [2]chtseng@ieee.org

***Abstract*— A new microwave oscillator-based microfluidic sensor is proposed in this paper for complex permittivity measurement. A modified coplanar strip resonator is proposed as the permittivity sensing device and frequency-selective element for the oscillator design. It can concentrate the sensing electric field with a distribution consistent with the microfluidic channel. As the test liquids are placed in the sensing region, the oscillation frequency and output power are measured for complex permittivity computation. The 23-μL water-ethanol mixtures with ethanol volume fractions of 10% to 70% in increments of 20% are used as the test liquids to evaluate the sensor performance. Compared with the results obtained from the commercial dielectric probe, the maximum errors of the dielectric constant and loss tangent measured by the proposed microfluidic sensor are 9.45% and -8.84%, respectively.**

***Keywords*— radio-frequency microfluidic sensors, complex permittivity measurement, radio-frequency permittivity sensors, liquid dielectric sensors, modified coplanar strip resonator (MCSR).**

I. Introduction

Characterization of liquid permittivity in the microwave/millimeter-wave range is an effective approach to estimating the concentration of aqueous solutions and classifying the type of liquid. The permittivity measurement technique has been increasingly applied in food industrial [1], biological [2], and pharmaceutical [3] fields. Combined with microfluidics, one can precisely control the test liquid volume in a micro-litter scale for advanced applications on the microscopic scale, such as biological cell investigation [4], [5]. Over the past decade, various new microwave microfluidic sensors have been proposed in the microwave research community and are mainly categorized into the passive-type [6], [7], [8], [9] and active-type [10], [11], [12], [13], [14].

The recently developed passive-type sensors, such as the split-ring resonator (SRR) [6], microstrip LC resonator [7], complementary split-ring resonator (CSRR) [8], and substrate integrated waveguide (SIW) cavity [9], mainly focus on miniaturizing the circuit size, reducing the volume requirement of the test liquid, and improving the sensitivity. However, a vector network analyzer (VNA) is essential to build a complete sensor system for complex permittivity measurement. It is bulky, expensive, and impractical for the internet of things (IoT) or sensor network applications. Therefore, the active-type sensors using the correlators with capacitive sensors [10], the in-phase and quadrature-phase (IQ) down-conversion mixers with a capacitive sensor

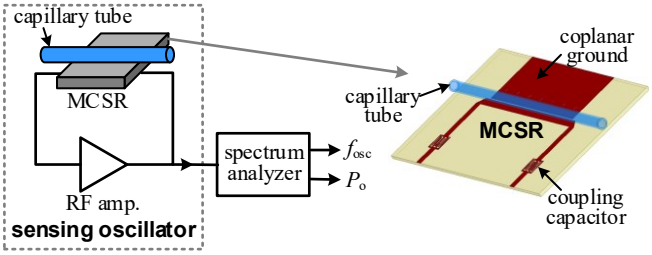

Fig. 1. System block diagram of the proposed microfluidic permittivity sensor.

[11], a sensing voltage-controlled oscillator (VCO) with a phase-locked loop (PLL) [12], a VCO-based sensor with both sensing and reference VCOs [13], and a frequency-locked-loop (FLL) sensor with a frequency discriminator [14], have been proposed to get rid of using a VNA.

Although the CMOS sensing oscillators for dielectric constant measurement (real part of relative permittivity) have been proposed in [12], [13], they are only suitable to detect the test liquid in a tiny sensing area over the sensing capacitor structure of the packaged chip. For some microfluidic applications, the sensing area with a uniform electric-field distribution is required to have a layout pattern similar to that of the microfluidic channel or chamber to improve the sensor sensitivity. In addition, the limited measurement capability, i.e., only measuring the real part of permittivity, has difficulty characterizing the complete liquid properties.

This study proposes a new microwave microfluidic sensor using a sensing oscillator with a modified coplanar strip resonator (MCSR) to have a more flexible sensing field distribution for complex permittivity measurement. The system block diagram of the proposed permittivity sensor is shown in Fig. 1. A capillary tube with the test liquid is used to emulate a microfluidic channel. The inset figure shows that the tube is then placed on the MCSR along with the gap structure between the strip line and the coplanar ground to experience the electric field. In this sensor configuration, the MCSR is used as a sensing device and treated as the frequency-selective component for the feedback-loop oscillator design. A spectrum analyzer then measures the sensing oscillator to acquire the oscillation frequency and output power as different test liquids are placed on the MCSR.

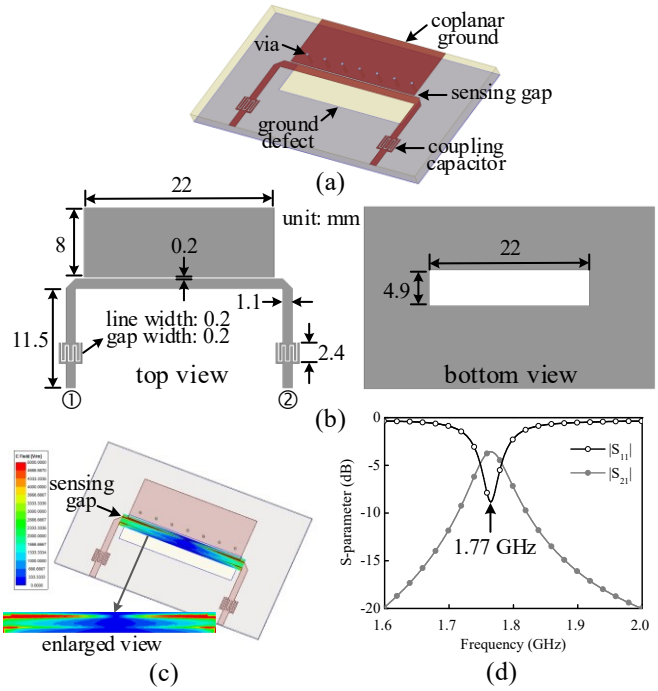

Fig. 2. (a) Three-dimensional structure and (b) physical dimensions of the proposed modified coplanar strip resonator (MCSR) with its (c) electric-field distribution and (d) measured S-parameters.

II. Permittivity Sensor Design

Referring to the sensor configuration shown in Fig. 1, the MCSR simultaneously plays the role of a liquid sensing device and a frequency-selective resonator for the oscillator design. Fig. 2 (a) shows the three-dimensional structure of the MCSR with the physical dimensions indicated in Fig. 2 (b). It is designed at 1.8 GHz on a 20-mil RO4003C substrate, with a dielectric constant of 3.55 and a loss tangent of 0.0027. The MCSR is mainly a half-wavelength transmission-line (TL) resonator, and a portion of the TL is replaced by a conductor strip with a coplanar ground plane. In addition, the ground-defected structure on the bottom conductor layer is placed beneath the strip line and coplanar ground to concentrate the electric-field distribution into the sensing gap. The radio-frequency (RF) energy couples into this resonator via bilateral interdigital capacitors. Fig. 2 (c) shows the electric-field distribution simulated by the ANSYS High-Frequency Structure Simulator (HFSS) on the virtual plane, which is placed on the surface of MCSR. As expected, the electric field concentrates on the sensing gap. Since the appearance of the electric-field sensing area of the MCSR is similar to the capillary tube shown in Fig. 1, it provides an advantage to penetrate a stronger electric field into the test tube for sensitivity improvement. The measured S-parameters of the MCSR are shown in Fig. 2 (d), and the resonance frequency is located at 1.77 GHz.

Based on the feedback-loop oscillator configuration, the MCSR sensing oscillator is designed according to the design procedures in [15] and fabricated on a RO4003C substrate. Fig. 3 (a) shows the circuit photograph of the proposed sensor. The design comprises the MCSR, an RF amplifier, and connecting microstrip lines. The MCSR has been designed as shown in Fig. 2. An Infineon BFP405 bipolar junction transistor (BJT), biased at $V_{cc} = 2.2$ V and $I_c = 10$ mA, is used as an amplifier to compensate the loss contributed from the MCSR and satisfy the loop gain requirement of the Barkhausen oscillation criterion. Similarly, the connecting microstrip lines were designed to fulfill the loop phase requirement. The output spectrum measured by the Angilent spectrum analyzer N9010A is shown in Fig. 3 (b). The oscillation frequency of the MCSR oscillator is located at 1.82 GHz, with an output power of 2.96 dBm.

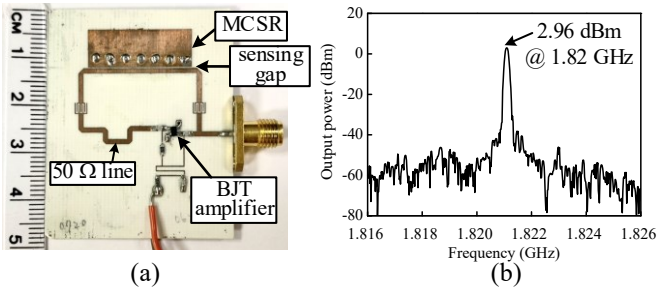

Fig. 3. (a) Circuit photograph of the MCSR sensing oscillator and (b) its measured output spectrum.

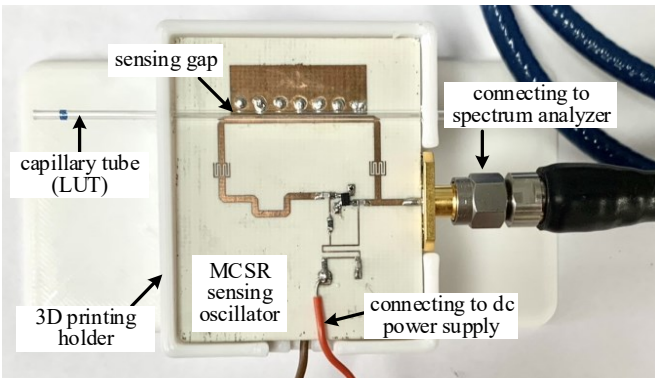

Fig. 4. Permittivity measurement setup of the developed microfluidic sensor.

III. Experimental Results

A. Sensor Calibration

Fig. 4 shows the permittivity measurement setup for the proposed microfluidic sensor. A three-dimensional (3D) printing plastic holder is fabricated to fix the position of the capillary tube stably on the sensing gap. The sensor output is connected with the Agilent EXA N9010A spectrum analyzer to acquire the oscillation frequency and output power. Before performing the permittivity measurement, one should first calibrate the proposed microfluidic sensor to obtain the equations relating the measured oscillation frequency, f_{osc}, and output power, P_o, to the dielectric constant, ε_r, and loss tangent, $\tan\delta$, respectively. Here, the complex relative permittivity ε of the liquid under test (LUT) is defined as

Table 1. Measured f_{osc} and P_o of Proposed Sensor for Different Water-Ethanol Calibration Liquids

EVF (%)	f_{osc} (GHz)	P_o (dBm)	cal. ε_r	cal. $tan\delta$
0	1.78547	3.64	77.76	0.0868
20	1.78591	3.60	66.16	0.1256
40	1.78679	3.54	53.74	0.2021
60	1.78756	3.48	39.02	0.3104
80	1.79053	3.42	24.40	0.4975

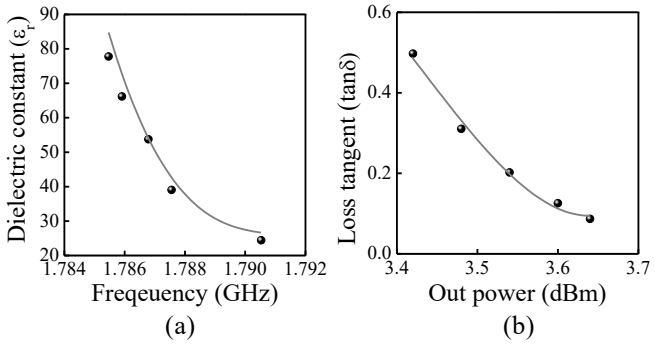

Fig. 5. (a) Calibration ε_r versus f_{osc} and (b) Calibration $\tan\delta$ versus P_{out} with fitting polynomial curves.

$\varepsilon = \varepsilon' - j\varepsilon''$. ε' is the real part of the complex relative permittivity, referred to as "dielectric constant", ε_r. Moreover, the imaginary part of ε can be divided by ε' to define the loss tangent as $\tan\delta = \varepsilon''/\varepsilon'$ [16]. Referring to Fig. 2 (b), since the length of the sensing gap is 22 mm, and the inner radius of the capillary tube is 1.15 mm, the LUT volume for permittivity measurement is approximately 23 μL.

In this paper, the water-ethanol mixtures with ethanol volume fractions (EVF) of 0% to 80% in increments of 20%, i.e., 0%, 20%, 40%, 60%, and 80%, were used as the calibration liquids. After injecting the calibration liquids into the capillary tube, f_{osc} and P_o were measured and listed in Table 1. Since the sensor used a tiny near field to sense the test liquid and the frequency shift was about only 0.28% of the oscillation frequency, the sensing oscillator was still in the stable region in the measurement. According to the microfluidic oscillator sensors in [12], [13], [17], the oscillation frequency and output power variations for different LUTs can be further related to the real part of permittivity, ε_r, and loss tangent, $\tan\delta$, of the known calibration liquids, respectively. The complex permittivities of the calibration liquids, measured by the Keysight N1501A Dielectric Probe Kit in combination with the E5071C Vector Network Analyzer, were also summarized in Table 1 for performing the curve fitting. Fig. 5 (a) plots the calibration ε_r shown in Table 1 versus f_{osc} and fitted by a 3-order polynomial equation as

$$\varepsilon_r = -12.27\left(\frac{f_{osc}-1.78846}{0.003455}\right)^3 + 28.41\left(\frac{f_{osc}-1.78846}{0.003455}\right)^2 - 24.87\left(\frac{f_{osc}-1.78846}{0.003455}\right) + 34 \quad (1)$$

Similarly, Fig. 5 (b) plots the calibration $\tan\delta$ shown in Table 1 versus P_o and fitted by a polynomial curve expressed as

$$\tan\delta = 0.06552\left(\frac{P_o-3.485}{0.148}\right)^3 + 0.07113\left(\frac{P_o-3.485}{0.148}\right)^2 - 0.3604\left(\frac{P_o-3.485}{0.148}\right) + 0.3189 \quad (2)$$

Hence, based on (1) and (2), the measured f_{osc} and P_o of the proposed microfluidic permittivity sensor successfully relate to the ε_r and $\tan\delta$ of the test liquid.

Table 2. Measurement Comparisons of Water-Ethanol Mixtures for Proposed Sensor and Commercial Dielectric Probe

EVF (%)	ε_r	ref. ε_r	error	$tan\delta$	ref. $tan\delta$	error
10	78.52	71.74	9.45%	0.0991	0.0974	1.75%
30	60.30	60.16	0.23%	0.1478	0.1621	-8.84%
50	44.01	46.78	-5.92%	0.2604	0.2505	3.97%
70	28.01	30.55	-8.32%	0.4072	0.3813	6.79%

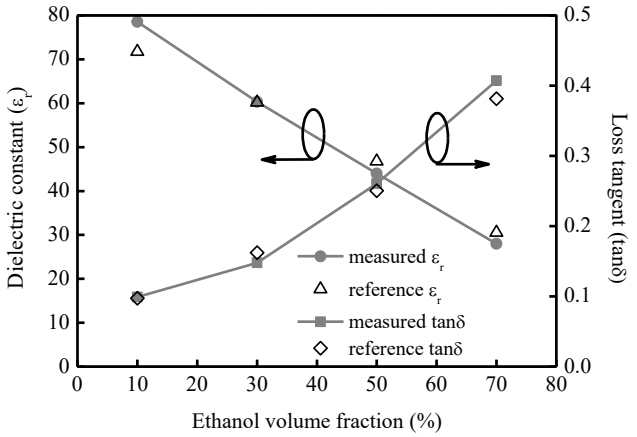

Fig. 6. Measured ε_r and $\tan\delta$ of the water-ethanol mixtures using the proposed microfluidic sensor.

B. Permittivity Measurement

To verify the proposed microfluidic permittivity sensor, the water-ethanol mixtures with EVFs from 10% to 70% in increments of 20%, namely 10%, 30%, 50%, and 70%, were used as the LUTs. By injecting the LUTs into the capillary tube on the MCSR shown in Fig. 4, one can acquire the f_{osc} and P_o corresponding to the liquid concentrations from the spectrum analyzer. The measured ε_r and $\tan\delta$ results can be calculated by substituting the measured f_{osc} and P_o into (1) and (2). Fig. 6 showed the measured ε_r and $\tan\delta$. In addition, the reference results measured by the dielectric probe kit were illustrated for comparison. The exact measured values using the proposed microfluidic permittivity sensor and the dielectric probe kit are listed in Table 2. The maximum errors of ε_r and $\tan\delta$ are 9.45% and -8.84%, respectively. The complex permittivities measured by the proposed microfluidic sensor are in good agreement with those obtained by the dielectric probe kit.

Table 3 shows the measurement performance comparisons of active liquid permittivity sensors from the published literature and this work. Since the sensors use the LUTs with a larger volume (100-250 μL) in [10], [11], [14] and a narrower ε_r range (about 2.5-25) in [10], [11], [12], [13] to evaluate

Table 3. Performance Comparison of Active Liquid Permittivity Sensors from Literature and the Proposed Microfluidic Permittivity Sensor

	Frequency (GHz)	Sensor technology	LUT (Volume)	ε_r error	$tan\delta$ or ε'' error
[10]	1-8	capacitive sensor with correlators	ethyl acetate (250 μL)	$< 1.32\%$	–
[11]	0.5-3	interdigital capacitor with IQ mixers	isopropanol-methanol (150 μL)	$< 1.5\%$	$< 1.5\%$ (ε'')
[12]	7-9	PLL-based sensing oscillator	6 different chemicals (20 μL)	$< 3.5\%$	–
[13]	10.4	PLL-based sensing oscillator	methanol-ethanol (20 μL)	$< 1.5\%$	–
[14]	5.798	FLL-based sensor	water-ethanol (100 μL)	$< 2.66\%$	$< 9.94\%$ ($\tan\delta$)
This work	1.78	oscillator-based sensor	water-ethanol (23 μL)	$< 9.45\%$	$< 8.84\%$ ($\tan\delta$)

the measurement performance, the accuracy of measuring ε_r is better than this work. Although the PLL-based sensors in [12] and [13] can improve the sensitivity and need a smaller LUT volume simultaneously, they did not have the capability of measuring ε'' or $\tan\delta$.

IV. Conclusion

A new microwave oscillator-based microfluidic sensor was proposed, designed, and experimentally verified to measure the complex permittivities of water-ethanol mixtures. To flexibly fit the layout pattern of the microfluidic channel, an MCSR sensing device is proposed in this paper to concentrate the electric field in a narrow gap and treated as a frequency-selective element for the sensing oscillator design. The maximum measured errors of ε_r and $\tan\delta$ of the water-ethanol mixtures were well controlled below 10% compared to the results measured by a commercial dielectric probe kit. In the future, a frequency demodulator will be developed to transfer the sensing oscillator's the frequency shifts and power variations to I/Q channel voltages for data manipulation.

Acknowledgment

This work was supported by the Ministry of Science and Technology of Taiwan under Grant MOST 110-2221-E-011-044-MY2.

References

[1] M. Kent, A. Peymann, C. Gabriel, and A. Knight, "Determination of added water in pork products using microwave dielectric spectroscopy," *Food Control*, vol. 13, no. 3, p. 143–149, Apr. 2002.

[2] J. C. Booth, J. Mateu, M. Janezic, J. Baker-Jarvis, and J. A. Beall, "Broadband permittivity measurements of liquid and biological samples using microfluidic channels," in *IEEE MTT-S Int. Microwave Symp. Dig.*, San Francisco, CA, USA, Jun. 2006, pp. 1750–1753.

[3] E. Benoit, O. Prot, P. Maincent, and J. Bessiere, "Applicability of dielectric measurements in the field of pharmaceutical formulation," *Bioelectrochem. Bioenerget.*, vol. 40, no. 2, p. 175–179, Feb. 1996.

[4] K. Grenier *et al.*, "Recent advances in microwave-based dielectric spectroscopy at the cellular level for cancer investigations," *IEEE Trans. Microw. Theory Techn.*, vol. 61, pp. 2023–2030, May 2013.

[5] F. Artis *et al.*, "Microwaving biological cells: Intracellular analysis with microwave dielectric spectroscopy," *IEEE Microw. Mag.*, vol. 16, pp. 87–96, May 2015.

[6] A. A. Abduljabar, D. J. Rowe, A. Porch, and D. A. Barrow, "Novel microwave microfluidic sensor using a microstrip split-ring resonator," *IEEE Trans. Microw. Theory Techn.*, vol. 62, no. 3, pp. 679–688, Mar. 2014.

[7] A. Ebrahimi, J. Scott, and K. Ghorbani, "Ultrahigh-sensitivity microwave sensor for microfluidic complex permittivity measurement," *IEEE Trans. Microw. Theory Techn.*, vol. 67, no. 10, pp. 4269–4277, Oct. 2019.

[8] E. L. Chuma, Y. Iano, G. Fontgalland, and L. L. B. Roger, "Microwave sensor for liquid dielectric characterization based on metamaterial complementary split ring resonator," *IEEE Sensors J.*, vol. 18, no. 24, pp. 9978–9983, Dec. 2018.

[9] G. M. Rocco *et al.*, "3-D printed microfluidic sensor in SIW technology for liquids' characterization," *IEEE Trans. Microw. Theory Techn.*, vol. 68, no. 3, pp. 1175–1184, Mar. 2020.

[10] A. A. Helmy and K. Entesari, "A 1-8 GHz miniaturized spectroscopy system for permittivity detection and mixture characterization of organic chemicals," *IEEE Trans. Microw. Theory Techn.*, vol. 60, no. 12, pp. 4157–4170, Dec. 2012.

[11] A. A. Helmy, S. Kabiri, M. M. Bajestan, and K. Entesari, "Complex permittivity detection of organic chemicals and mixtures using a 0.5-3 GHz miniaturized spectroscopy system," *IEEE Trans. Microw. Theory Techn.*, vol. 61, no. 12, pp. 4646–4658, Dec. 2013.

[12] A. A. Helmy *et al.*, "A self-sustained CMOS microwave chemical sensor using a frequency synthesizer," *IEEE J. Solid-State Circuits*, vol. 47, no. 10, pp. 2467–2483, Oct. 2012.

[13] O. Elhadidy *et al.*, "A CMOS fractional-N PLL-based microwave chemical sensor with 1.5% permittivity accuracy," *IEEE Trans. Microw. Theory Techn.*, vol. 61, no. 9, pp. 3402–3416, Sep. 2013.

[14] C.-H. Tseng and C.-Y. Yang, "Novel microwave frequency-locked-loop-based sensor for complex permittivity measurement of liquid solutions," *IEEE Trans. Microw. Theory Techn.*, vol. 70, no. 10, pp. 4556–4565, Oct. 2022.

[15] C.-H. Tseng and C.-L. Chang, "Design of low phase-noise microwave oscillator and wideband VCO based on microstrip combline bandpass filters," *IEEE Trans. Microw. Theory Techn.*, vol. 60, no. 10, pp. 3151–3160, Oct. 2012.

[16] D. M. Pozar, *Microwave Engineering*, 3rd ed. New York, NY, USA: Wiley, 2005.

[17] V. Lammert *et al.*, "A k-band complex permittivity sensor for biomedical applications in 130-nm SiGe BiCMOS," *IEEE Trans. Circuits Syst., II, Exp. Briefs*, vol. 66, no. 10, pp. 1628–1632, Oct. 2019.